Journal of Biomechanics 43 (2010) 2637–2640

Contents lists available at ScienceDirect

Journal of Biomechanics

journal homepage: www.elsevier.com/locate/jbiomech
www.JBiomech.com

Short communication

Full field strain measurements of collagenous tissue by tracking fiber alignment through vector correlation

Kyle P. Quinn, Beth A. Winkelstein*

Spine Pain Research Laboratory, Departments of Bioengineering & Neurosurgery, University of Pennsylvania, 240 Skirkanich Hall, 210 S. 33rd St, Philadelphia, PA 19104-6321, USA

ARTICLE INFO

Article history:
Accepted 10 May 2010

Keywords:
Vector correlation
Strain
Feature tracking
Collagen fiber
Polarized light

ABSTRACT

Full field strain measurements of biological tissue during loading are often limited to the quantification of fiduciary marker displacements on the tissue surface. These marker measurements can lack the necessary spatial resolution to characterize non-uniform deformation and may not represent the deformation of the load-bearing collagen microstructure. To overcome these potential limitations, a method was developed to track the deformation of the collagen fiber microstructure in ligament tissue. Using quantitative polarized light imaging, fiber alignment maps incorporating both direction and alignment strength at each pixel were generated during facet capsular ligament loading. A grid of virtual markers was superimposed over the tissue in the alignment maps, and the maximization of a vector correlation calculation between fiber alignment maps was used to track marker displacement. Tracking error was quantified through comparisons to the displacements of excised ligament tissue ($n=3$); separate studies applied uniaxial tension to isolated facet capsular ligament tissue ($n=4$) to evaluate tracking capabilities during large tissue deformations. The average difference between virtual marker and tissue displacements was 0.07 ± 0.06 pixels. This error in marker location produced principal strain measurements of $1.2 \pm 1.6\%$ when markers were spaced 4 pixels apart. During tensile tissue loading, substantial inhomogeneity was detected in the strain field using vector correlation tracking, and the location of maximum strain differed from that produced by standard tracking techniques using coarser meshes. These findings provide a method to directly measure fiber network strains using quantitative fiber alignment data, enabling a better understanding of structure–function relationships in tissues at different length scales.

1. Introduction

Quantifying the local deformation of a biological tissue during loading is often required in biomechanical studies, but can be technically challenging. Recent automated image analysis techniques take advantage of the spatial variability in a tissue's optical or acoustic properties and utilize cross-correlation techniques to track displacements based on the unique features of the surrounding tissue (Korstanje et al., 2010; Michalek et al., 2009; Snedeker et al., 2006). In cases where tissue lacks a measurable spatial pattern, fiduciary markers or textures have been applied to the tissue surface to enable feature tracking (Derwin et al., 1994; Gilchrist et al., 2007; Siegmund et al., 2001). However, those techniques are often limited to measuring only surface strains, which may differ from the stains experienced by the load-bearing collagen microstructure throughout the thickness of a tissue.

Measuring the local deformation of a collagen fiber network within a tissue can be accomplished by utilizing the linear birefringence of collagen fibers (Vidal et al., 1982). Recently, aortic valve deformation was tracked using the patterns produced from the interference colors created by collagen birefringence, fiber alignment, and tissue thickness during the transmission of polarized light (Doehring et al., 2009). Tracking interference color patterns in that study enabled local collagen network strains to be measured. We hypothesized that enhanced tracking accuracy and improved strain field resolution could be achieved by quantifying the fiber direction and alignment strength at each pixel prior to tracking. Here, we present a technique to measure local collagen network deformations in ligament using the fiber alignment maps acquired through quantitative polarized light imaging.

2. Methods

2.1. Polarized light imaging system

A quantitative polarized light imaging (QPLI) system capable of acquiring pixel-wise collagen fiber alignment maps during continuous tissue loading has

* Corresponding author. Tel.: +1 215 573 4589; fax: +1 215 573 2071.
E-mail address: winkelst@seas.upenn.edu (B.A. Winkelstein).

0021-9290/$ - see front matter © 2010 Elsevier Ltd. All rights reserved.
doi:10.1016/j.jbiomech.2010.05.008

been previously described (Quinn and Winkelstein, 2008; Tower et al., 2002). In this system, light is transmitted through a rotating linear polarizer and a tissue sample before entering a lens outfitted with a circular analyzer. The intensity of light measured by the camera at each pixel during the polarizer rotation is fit to a harmonic equation. Based on the linear birefringence of the collagen fibers, the average fiber direction and retardation (i.e. strength of alignment) at each pixel can be determined from the phase and amplitude of the harmonic response, respectively (Tower et al., 2002).

2.2. Vector correlation tracking algorithm

A vector correlation approach previously used to localize microstructural damage in ligament tissue (Quinn and Winkelstein, 2009; Quinn et al., in press) was employed using Matlab (Mathworks; Natick, MA) to track the deformation of ligament tissue based on its fiber alignment. At each pixel in the fiber alignment maps, the axial fiber direction (α) and retardation (δ) values were transformed into an alignment vector with an orientation of 2α and length of $\sin(\delta)$. A grid of virtual markers spaced 4 pixels apart was superimposed over the first alignment map generated by the QPLI system. For each virtual marker, the fiber alignment from a 9×9 window of pixels centered around the virtual marker was used as the set of reference vectors for tracking the virtual marker (Fig. 1). Although virtual markers were spaced 4 pixels apart, the true resolution of the local deformation measurements was limited by the 9×9 pixel window used to track each marker. The reference alignment vectors for each virtual marker from the initial map were correlated with corresponding alignment vector sets generated from windows in the next alignment map. The vector correlation values in the second alignment map were determined within a 13×13 search window centered about the location of the virtual marker in the initial map (Fig. 1). The search window size did not affect tracking accuracy, but was selected to ensure it encapsulated all marker displacements. A two-dimensional spline interpolation of the 13×13 array of vector correlation values was performed within the search window to identify the location of the maximum correlation with 0.05 pixel resolution. The Cartesian coordinates of the location of maximum correlation were then taken as the temporary position of the virtual marker in the next map (labeled B' in Fig. 1).

To enhance the accuracy of the virtual marker displacements between each map, tracking was also performed in reverse at each step. Once the location of a virtual marker (B') was identified by tracking forward to the next frame, the alignment surrounding that location was used to track backwards to the previous frame and identify the former location of the marker (A' in Fig. 1b). An average of the marker's displacements during forward and backward tracking ($d_{AB'}$ and $d_{B'A'}$ in Fig. 1) was then used to define the displacement between frames and identify the final marker location in the next frame (B). This approach also allowed an assessment of error in the tracking method at each step. If the distance between a virtual marker's actual previous location (A in Fig. 1) and the location predicted by tracking forward and back (A' in Fig. 1) was greater than 2 pixels, the marker was removed from subsequent tracking and analysis. A two-pixel threshold for marker removal was a conservative metric that only eliminated markers in regions without measurable fiber alignment. To minimize the propagation of error in the marker position, the reference set of alignment vectors used to track forward was retained throughout multiple steps until the maximum vector correlation between maps for that marker decreased below 0.9 and the alignment surrounding the marker in that frame was used as the new reference vector set.

2.3. Strain field measurements

Using the grid of virtual markers constructed in the first alignment map, a mesh of elements was generated through Delaunay triangulation. Matlab code previously used to calculate Lagrangian strain in four-node shell elements (Quinn and Winkelstein, 2008) was modified to compute strain in each of the triangular elements in every alignment map using the virtual marker displacements. Principal strain was determined from the maximum eigenvalue of the derived strain tensor of each element, and a full field strain map was defined with nodal values averaged.

2.4. Validation and comparison to other tracking techniques

To assess error in the tracking algorithm, excised facet capsular ligaments ($n=3$) were placed on glass slides that were rigidly fixed to the crosshead of an Instron 5865 (Instron, Norwood, MA). A 2.5 mm vertical crosshead displacement was applied at a rate of 0.40 mm/s, with displacement data acquired at 1 kHz. A Phantom v9.1 camera (Vision Research; Wayne, NJ) acquired images at 500 Hz with a resolution of 18.52 pixels/mm as the linear polarizer rotated at 750 rpm. Alignment maps were generated from every 20 frames, and the acquisition parameters were selected to ensure that tissue displacement between maps was less than 0.3 pixels, which enabled continuous tissue loading. The absolute differences in the displacements between the Instron crosshead and the virtual markers from vector correlation tracking were computed. The ligament tissue was fixed to the slides so that it would not deform during translation, and the measured principal strain of tissue on the translated slide was calculated to assess the error in strain measurements using this tracking technique.

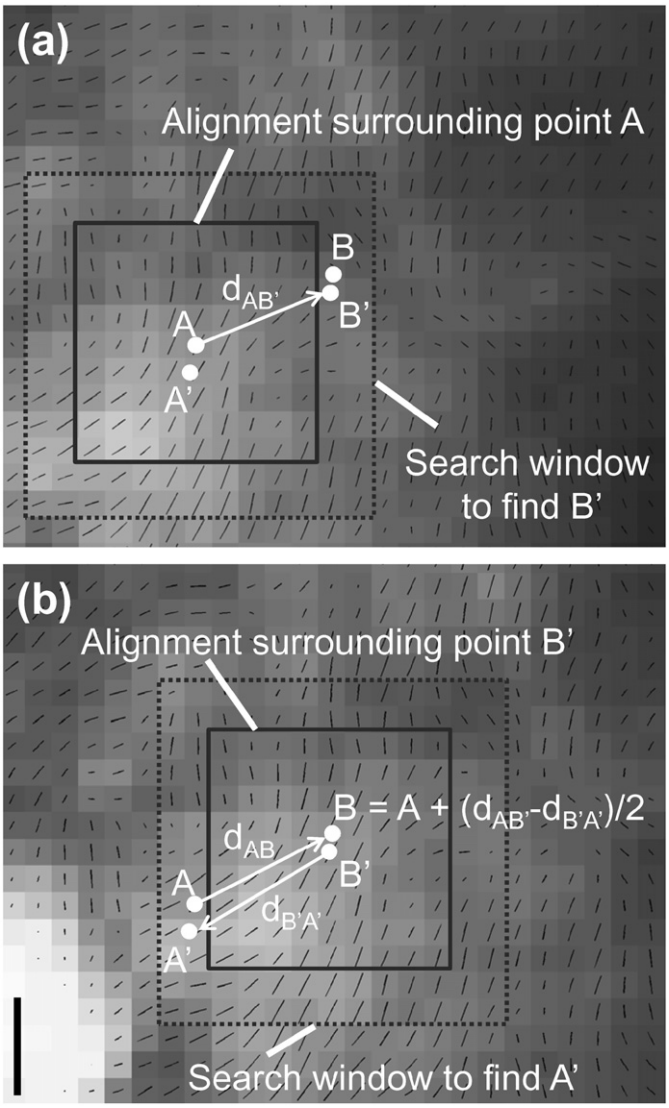

Fig. 1. Schematic of the vector correlation tracking process between two fiber alignment maps. (a) The displacement of the fiber alignment (black lines) surrounding point A between alignment maps is initially determined by identifying the location of the maximum vector correlation (point B') with the alignment in the next frame within a search window. (b) Using the fiber alignment surrounding point B', the location of point B' is tracked back to a location (A') in the initial alignment map. A combination of the forward ($d_{AB'}$) and backward ($d_{B'A'}$) displacements is then used to define the displacement (d_{AB}) from point A to point B. The scale bar represents 0.2 mm.

To evaluate the ability of the vector correlation technique to measure large tissue deformations, intact facet capsular ligaments ($n=4$) were loaded until visible tissue damage was induced. Vector correlation tracking was performed and virtual marker locations were compared to the location of fiduciary marks placed on the surface of the ligaments. The locations of fiduciary marks were digitized manually and also tracked using a standard intensity-based feature tracking program (ProAnalyst; Xcitex, Cambridge, MA). In the center of the samples, where fiber alignment surrounding the fiduciary marks could be measured, the locations of fiduciary marks ($n=15$ total) defined by both digitization and ProAnalyst were compared with vector correlation tracking measurements. The vector correlation tracking technique was not directly compared to tracking techniques that require the application of a random speckle pattern because these patterns would attenuate a substantial amount of the light transmission required to measure fiber alignment. Accordingly, principal strain fields were compared using vector correlation and the relatively coarser fiduciary mark tracking data.

3. Results and discussion

The average virtual marker ($n=854$ from 3 tests) displacement derived from the vector correlation tracking was 46.38 ± 0.10 pixels, after a 2.5 mm (46.38 pixels) displacement of the Instron crosshead (Fig. 2). The average absolute difference between marker displacements and the crosshead displacement was 0.07 ± 0.06 pixels. Error in the virtual marker locations at 2.5 mm produced an average first principal strain of 0.012 ± 0.016 from all 1508 elements (Fig. 2).

During tensile loading of facet capsular ligament tissue, the average difference in the displacements of the virtual markers and the digitized fiduciary markers was -0.24 ± 0.98 pixels in the x-direction and 0.17 ± 1.18 pixels in the y-direction. This variability in marker positions suggested that the systematic error between digitization and vector correlation tracking was less than 0.30 pixels; random error produced an average distance of 1.39 ± 0.61 pixels between marker locations measured by the two techniques. The differences in marker position could be attributable to either error in the vector correlation tracking and digitization processes or actual differences between deformation of the collagen microstructure and the surface of the ligament. By comparison, the average distance between the digitized marker location and that location determined by feature tracking using ProAnalyst was 1.67 ± 0.57 pixels, and the average distance between the vector correlation and feature tracking was 1.75 ± 0.61 pixels. In the strain fields produced by tracking virtual markers initially spaced 4 pixels apart, the mean first principal strain was 0.503 ± 0.238 at the point of ligament damage, which was substantially greater than the mean error of the strain measurements (0.012 ± 0.016). The strain fields with vector correlation tracking revealed inhomogeneity in the deformation of the tissue that was not previously detectable with coarser resolutions of 21.8 ± 5.6 pixels using fiduciary marker tracking (Fig. 3).

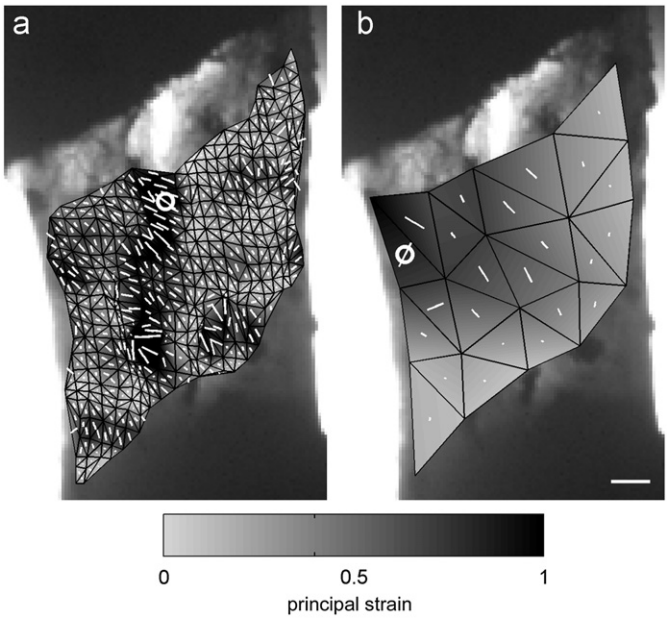

Fig. 3. Principal strain fields produced by (a) vector correlation tracking and (b) fiduciary mark tracking at 2.99 mm of displacement during tensile loading of a facet capsular ligament sample. The location of maximum principal strain, indicated by the circles in (a) and (b), differs between tracking techniques, and is located just below the site of a hole developing in the tissue with the vector correlation tracking method. Principal strain directions for each element are indicated by the white vectors in both plots. The scale bar in (b) represents 1 mm and also applies to (a).

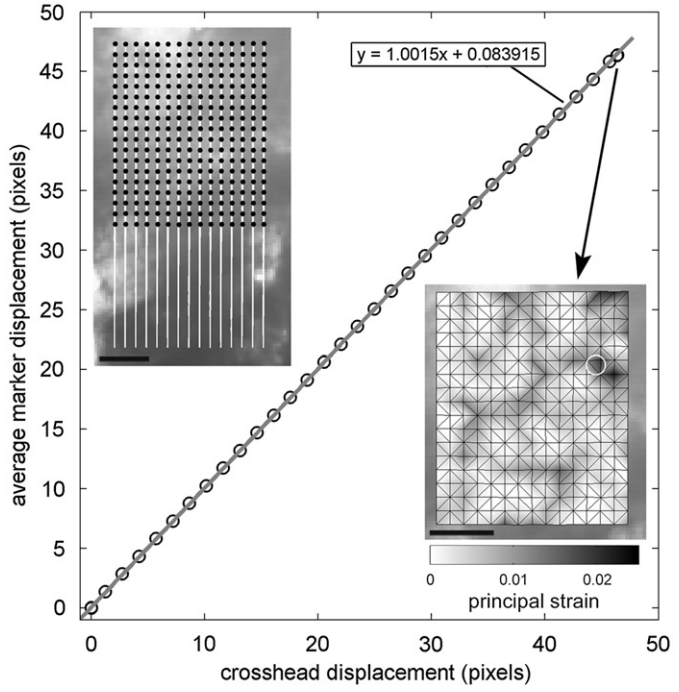

Fig. 2. Error analysis of the vector correlation tracking technique. The average virtual marker displacement follows the displacement of the Instron crosshead during a 2.5 mm translation of ligament tissue. The paths of the virtual markers were nearly identical to each other (left inset) and produced an average principal strain of 0.007 ± 0.009 at 2.5 mm in this test (right inset). The location of the element with the maximum principal strain (0.042) is identified by the circle in the inset on the right. Each scale bars in the insets represent 1 mm.

This study using vector correlation tracking demonstrates a method that directly measures the deformation of the load-bearing collagen microstructure of tissue. Full field principal strain measurements were made with a mean error of 1.2% in strain with virtual markers spaced 4 pixels apart. Local tissue displacement was measured by tracking quantitative fiber alignment data within a 9×9 pixel window, which improved the strain field resolution compared to similar polarized light-based tracking techniques based on interference colors (Doehring et al., 2009). With collagen fiber orientations directly incorporated into the vector correlation tracking algorithm, this technique has the unique ability to relate local deformation with microstructural organization. Future work may help to identify the complex structure–function relationships of collagenous tissue at different length scales and provide more accurate strain thresholds for tissue injury.

Conflicts of interest statement

There were no conflicts of interest for any authors with any aspect of this study.

Acknowledgments

This material is based on work supported by and the National Science Foundation under Grant no. 0547451, and was also funded by support from the Catharine D. Sharpe Foundation and

the Defense University Research Instrumentation Program of the U.S. Army Research Office.

References

Derwin, K.A., Soslowsky, L.J., Green, W.D.K., Elder, S.H., 1994. A new optical system for the determination of deformations and strains: calibration characteristics and experimental results. Journal of Biomechanics 27, 1277–1285.

Doehring, T.C., Kahelin, M., Vesely, I., 2009. Direct measurement of nonuniform large deformations in soft tissues during uniaxial extension. Journal of Biomechanical Engineering 131, 061001.

Gilchrist, C.L., Witvoet-Braam, S.W., Guilak, F., Setton, L.A., 2007. Measurement of intracellular strain on deformable substrates with texture correlation. Journal of Biomechanics 40, 786–794.

Korstanje, J.H., Selles, R.W., Stam, H.J., Hovius, S.E.R., Bosch, J.G., 2010. Development and validation of ultrasound speckle tracking to quantify tendon displacement. Journal of Biomechanics 43, 1373–1379.

Michalek, A.J., Buckley, M.R., Bonassar, L.J., Cohen, I., Iatridis, J.C., 2009. Measurement of local strains in intervertebral disc anulus fibrosus tissue under dynamic shear: contributions of matrix fiber orientation and elastin content. Journal of Biomechanics 42, 2279–2285.

Quinn, K.P., Bauman, J.A., Crosby, N.D., Winkelstein, B.A. Anomalous fiber realignment during tensile loading of the rat facet capsular ligament identifies mechanically induced damage and physiological dysfunction. Journal of Biomechanics, in press, doi:10.1016/j.jbiomech.2010.03.032.

Quinn, K.P., Winkelstein, B.A., 2008. Altered collagen fiber kinematics define the onset of localized ligament damage during loading. Journal of Applied Physiology 105, 1881–1888.

Quinn, K.P., Winkelstein, B.A., 2009. Vector correlation technique for pixel-wise detection of collagen fiber realignment during injurious tensile loading. Journal of Biomedical Optics 14, 054010.

Siegmund, G.P., Myers, B.S., Davis, M.B., Bohnet, H.F., Winkelstein, B.A., 2001. Mechanical evidence of cervical facet capsule injury during whiplash: a cadaveric study using combined shear, compression, and extension loading. Spine 26, 2095–2101.

Snedeker, J.G., Pelled, G., Zilberman, Y., Gerhard, F., Müller, R., 2006. Endoscopic cellular microscopy for in vivo biomechanical assessment of tendon function. Journal of Biomedical Optics 11, 064010.

Tower, T.T., Neidert, M.R., Tranquillo, R.T., 2002. Fiber alignment imaging during mechanical testing of soft tissues. Annals of Biomedical Engineering 30, 1221–1233.

Vidal, B.C., Mello, M.L., Pimentel, E.R., 1982. Polarization microscopy and microspectrophotometry of Sirius Red, Picrosirius and Chlorantine Fast Red aggregates and of their complexes with collagen. Histochemical Journal 14, 857–878.